

# Arresting Cancer Proliferation by Small-Molecule Gene Regulation

Liliane A. Dickinson,<sup>1</sup> Ryan Burnett,<sup>1</sup> Christian Melander,<sup>1</sup> Benjamin S. Edelson,<sup>2</sup> Paramjit S. Arora,<sup>2</sup> Peter B. Dervan,<sup>2,\*</sup> and Joel M. Gottesfeld<sup>1,\*</sup>

<sup>1</sup>Department of Molecular Biology  
The Scripps Research Institute  
La Jolla, California 92037

<sup>2</sup>Division of Chemistry and Chemical Engineering  
California Institute of Technology  
Pasadena, California 91125

## Summary

A small library of pyrrole-imidazole polyamide-DNA alkylator (chlorambucil) conjugates was screened for effects on morphology and growth characteristics of a human colon carcinoma cell line, and a compound was identified that causes cells to arrest in the G2/M stage of the cell cycle. Microarray analysis indicates that the histone H4c gene is significantly downregulated by this polyamide. RT-PCR and Western blotting experiments confirm this result, and siRNA to H4c mRNA yields the same cellular response. Strikingly, reduction of H4 protein by >50% does not lead to widespread changes in global gene expression. Sequence-specific alkylation within the coding region of the H4c gene in cell culture was confirmed by LM-PCR. The compound is active in a wide range of cancer cell lines, and treated cells do not form tumors in nude mice. The compound is also active *in vivo*, blocking tumor growth in mice, without obvious animal toxicity.

## Introduction

The development of programmable, gene-specific reagents that block either mRNA transcription or translation is a major goal in chemistry, molecular biology, and medicine. Nucleic acid-based approaches that target DNA or RNA (such as antisense or triple helix-forming oligonucleotides or siRNA [1–3]) take advantage of the sequence selectivity afforded by base pairing and can effectively inhibit transcription or translation in cell culture. Similarly, engineered zinc finger peptides [4–7] that recognize unique sequences in the genome have been shown to modulate gene expression when these molecules are delivered to cells via gene transfection. However, nucleic acids suffer from poor cell permeability, and delivery strategies, such as viral vectors, must be used for effective gene silencing *in vivo* [8, 9].

Cell-permeable small molecules circumvent the need for delivery strategies, and a number of natural and synthetic compounds have been explored for their ability to regulate gene expression *in vitro* and in cell culture [10, 11]. The pyrrole-imidazole (Py-Im) polyamides are a class of small molecules that can be programmed to

bind a broad spectrum of DNA sequences [12, 13]. Base sequence specificity depends on side-by-side pairing of Py and Im rings in the minor groove of DNA (Table 1, [12, 13]). Polyamides are cell permeable, localize in the nucleus [14–16], bind their target sites in genomic DNA with affinities comparable to DNA binding transcription factors [17], and regulate gene expression by interfering with the transcription apparatus at promoter and enhancer elements [12, 13]. In contrast, polyamides bound within coding regions of genes do not present an obstacle to elongating RNA polymerase [18]; however, linkage of a DNA-modifying agent, such as nitrogen mustards [19, 20], duocarmycins [21–23], or pyrrolobenzodiazepines [24, 25], to a polyamide is expected to arrest transcription elongation at the polyamide binding site [26]. Polyamide-alkylator conjugates have been described that covalently react at predetermined sites in human genomic DNA, in the nuclei of live cells [17, 19]. Inhibition of transcription *in vitro* [26], as well as luciferase expression in mammalian cell culture transfection experiments, has been obtained with polyamide-alkylator (duocarmycin DU86) conjugates [23]. The cytostatic properties of hairpin polyamide-alkylator conjugates have been examined previously [27], but no studies have examined the effects of these compounds on genomic transcription. Here, we describe a polyamide-chlorambucil (Chl) conjugate that blocks cancer cell proliferation by downregulation of transcription of a specific gene that encodes a key component of cellular chromatin.

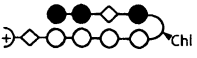
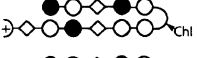

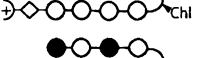
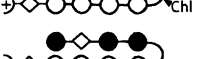
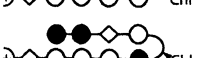
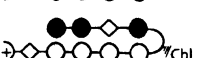
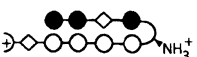
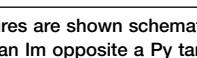
## Results

### Blocking Cancer Cell Proliferation with a Polyamide-Chlorambucil Conjugate

For our studies, we employed a highly tumorigenic human colon carcinoma cell line, SW620, that was derived from a lymph node metastasis [28]. We synthesized five different hairpin polyamides conjugated at the  $\alpha$  position of the hairpin turn amino acid with the nitrogen mustard Chl [17, 19, 29], and we screened these conjugates for their effects on the morphology of SW620 cells in culture. Each of these molecules had a different DNA sequence specificity afforded by the polyamide amino acid sequence (polyamides 1R-Chl to 5-Chl, Table 1) [12, 13], and each would be expected to alkylate adenine and guanine bases in the minor groove located adjacent to the polyamide recognition site [17, 19, 29]. Among the polyamides tested, microscopic inspection demonstrated that only 1R-Chl (Figure 1) altered the morphology of the cells (Figure 2A). Untreated SW620 cells are typically either round or spindle shaped, whereas incubation with polyamide 1R-Chl alters the morphology of these cells to an enlarged, flattened, and irregular shape. Concentrations as low as 250 nM induce the morphological change in 48 hr. Cells treated with this compound fail to divide; consequently, fewer treated cells are seen compared to the untreated cells. Nonetheless, cells treated with this polyamide are viable (>90% by trypan

\*Correspondence: dervan@its.caltech.edu (P.B.D.); joelg@scripps.edu (J.M.G.)

Table 1. Growth Arrest and Cell Morphology Change Requires the Sequence Specificity of **1R-Chl**

| Polyamide | Polyamide Structures  | Sequence      | Cell Morphology Change | Growth Arrest | Viability |
|-----------|---|---------------|------------------------|---------------|-----------|
| 1R-Chl    |  | 5'-WGGWGW-3'  | yes                    | yes           | +         |
| 2-Chl     |  | 5'-WGCWGW-3'  | no                     | no            | +         |
| 3-Chl     |  | 5'-WGCWGCW-3' | no                     | no            | +         |
| 4-Chl     |  | 5'-WGWWWW-3'  |                        | cytotoxic     |           |
| 5-Chl     |  | 5'-WGWGW-3'   |                        | cytotoxic     |           |
| 6-Chl     |  | 5'-WGWGGW-3'  | no                     | slight        | +         |
| 7-Chl     |  | 5'-WGGWCW-3'  | no                     | slight        | +         |
| 1S-Chl    |  | 5'-WGWGGW-3'  | no                     | no            | +         |
| 1R        |  | 5'-WGGWGW-3'  | no                     | no            | +         |

Polyamide structures are shown schematically (as in Figure 1), along with the predicted DNA target site for each polyamide [13], where W = A or T. Pairing of an Im opposite a Py targets a G•C base pair, whereas a Py opposite an Im targets a C•G base pair. The Py/Py,  $\beta$ /Py, and  $\beta$ / $\beta$  pairs are degenerate and target both A•T and T•A base pairs. Both the hairpin turn amino acid and the terminal  $\beta$ -Dp recognize A•T or T•A base pairs. With the exception of **1S-Chl**, all polyamides were synthesized with *R*-2,4-diaminobutyric acid as the turn amino acid. Morphology change was assessed as in Figure 2A, and growth arrest is based on cell counts. Viability was assessed by trypan blue exclusion and an ATP assay (see Supplemental Figure S1).

blue exclusion) and metabolically active (assessed by ATP levels; Supplemental Figure S1; see the Supplemental Data available with this article online). Thus, **1R-Chl** is a cytostatic, rather than a cytotoxic, agent in this cell line. Two polyamide conjugates that had the lowest sequence specificity of the tested compounds, **4-Chl** and **5-Chl**, were highly cytotoxic and were not studied further. These compounds are similar to conventional alkylators that target vast numbers of sites in the genome. **Chl** (at 0.5  $\mu$ M) is without effect on SW620 cell morphology or growth (Figure 2A), but it is cytotoxic at higher concentrations (Supplemental Figure S1).

After identification of **1R-Chl**, we probed the structural requirements for growth arrest with a second series of compounds (Table 1). We found that altering DNA sequence specificity by either scrambling the sequence of pyrrole and imidazole rings (**6-Chl** and **7-Chl**) or by inverting the chirality of the turn amino acid (**1S-Chl**, Figure 1) [30, 31] abolished the morphological change and growth arrest observed with **1R-Chl**. Furthermore, the parent polyamide **1R**, lacking **Chl**, was inactive. These experiments show that the morphological change and cytostatic properties of **1R-Chl** require both the alkylating moiety **Chl** and the sequence-specific DNA binding moiety of the polyamide, suggesting that these effects are due to sequence-specific DNA alkylation and concomitant gene silencing.

To test cell permeability and nuclear localization of the polyamides, we synthesized fluorescent analogs of active polyamide **1R-Chl** and inactive polyamide **1S-Chl**. Similar to the **Chl** conjugates, the fluorescent dye Bodipy FL was coupled to the  $\alpha$ -amino group of the turn

amino acid [14] (Figure 1). Using deconvolution microscopy, we observe that both **1R-bodipy** and **1S-bodipy** enter the nucleus of live, unfixed SW620 colon cancer cells (Supplemental Figure S2). To assess the mechanism of action of polyamide **1R-Chl**, we monitored the DNA content of untreated, **1R-Chl**-treated, and **1S-Chl**-treated SW620 cells by fluorescence-activated cell sorting (FACS) analysis after propidium iodide staining (Figure 2B). The DNA profiles of untreated and **1S-Chl**-treated cells were similar, with approximately 5%–7% of the cells in G2/M (4C DNA content), whereas treatment with polyamide **1R-Chl** increased the fraction of cells with a 4C DNA content to 43%. This finding indicates that polyamide **1R-Chl** arrests cells in the G2/M phase of the cell cycle. A small fraction of the **1R-Chl**-treated cells were apoptotic, as evidenced by less than a 2C DNA content. A time course experiment revealed that cell cycle arrest occurred approximately 2 days after polyamide treatment (data not shown), similar to the time required to observe the change in cell morphology described above. Upon longer exposure to the polyamide, increasing numbers of cells had a 4C DNA content, consistent with a block in the cell cycle at G2/M.

#### Gene Target of the Polyamide

The effects of polyamide treatment on genomic transcription were monitored by DNA microarray analysis by using Affymetrix high-density U133A arrays, which contain oligonucleotides representing  $\sim$ 18,000 human genes. SW620 cells were treated (in triplicate) with no polyamide, with **Chl**, or with polyamide **1R-Chl** or **1S-Chl** at a concentration of 0.5  $\mu$ M in culture medium

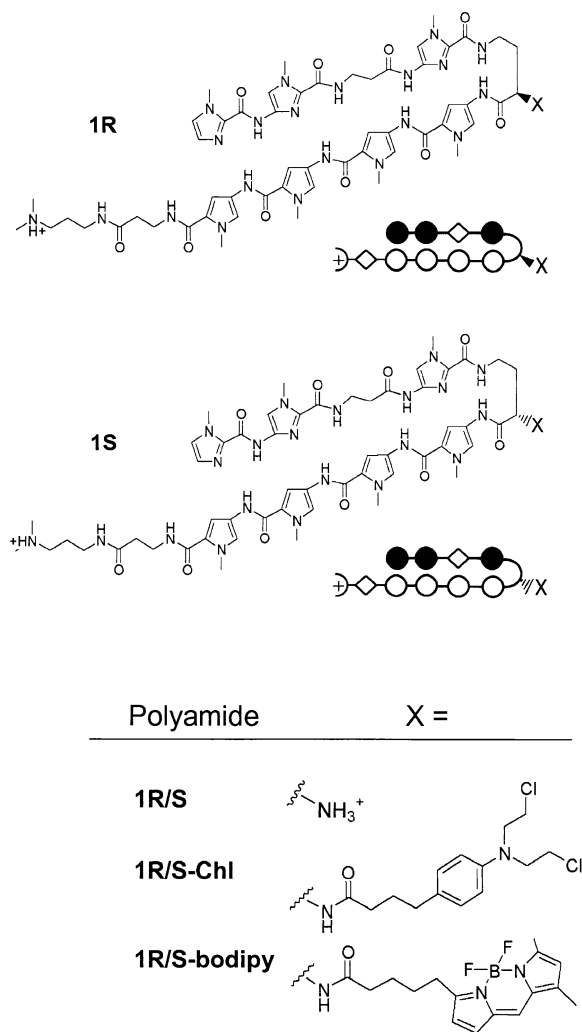


Figure 1. Polyamide Conjugate Structures

Structures of polyamides **1R**, **1S**, and **bodipy** and **Chl** conjugates (ImIm- $\beta$ -Im-(*R/S*-2,4-Daba<sup>bodipy/Chl</sup>)-PyPyPyPy- $\beta$ -Dp, where Py is pyrrole, Im is imidazole,  $\beta$  is  $\beta$ -alanine, Dp is dimethylaminopropylamine, and Daba is either *R*- or *S*-2,4-diaminobutyric acid). Polyamide structures are also represented schematically, where filled and open circles are Im and Py rings, respectively; diamonds are  $\beta$ -alanine; the curved line is *R* or *S*-2,4-diaminobutyric acid; and the semicircle with the plus sign is dimethylaminopropylamine.

for 72 hr (a sufficient time for growth arrest, described above). Total RNA was isolated, converted into fluorescent cRNA, and hybridized to the oligonucleotide microarrays. Figure 3A shows the number of genes that are up- and downregulated by each incubation condition. Whereas **Chl** affects the transcription of a large number of genes, the levels of transcription of a surprisingly limited number of genes were affected by polyamide-**Chl** treatment (77 genes upregulated and 35 downregulated for **1R-Chl**; Figure 3A and Supplemental Tables). Of the genes that were affected by **1R-Chl**, 23 genes were uniquely downregulated (Supplemental Table S1), and 70 genes were uniquely upregulated when compared to parent **1R**, **Chl**, and mirror image **1S-Chl**.

Of the specifically upregulated genes, only three

were increased in expression by 2-fold or more. These genes encode  $\beta$ -tubulin (GenBank accession number NM\_001069), epithelial membrane protein 1 (GenBank accession number NM\_001423), and CD24 antigen (GenBank accession number NM\_013230). Only the gene encoding member G of the nucleosomal histone H4 family (GenBank accession number NM\_003542; *H4c* gene) was uniquely downregulated by a threshold value of at least 2-fold. Downregulation of histone H4 could reasonably account for the growth effects observed with **1R-Chl** (see Discussion). Affymetrix U133A chips contain oligonucleotides representing all members of the H4 gene family; however, only the transcription of *H4c* was affected. *H4c* is the most abundantly transcribed H4 gene in untreated SW620 cells and accounts for  $\sim 70\%$  of total H4 mRNA. Real-time quantitative reverse transcriptase PCR (RT-PCR) verified that **1R-Chl** downregulates this gene  $\sim 2$ -fold. We next examined the level of histone H4 protein in polyamide-treated and control SW620 cells by Western blot analysis with an antibody to H4 (Figure 3B). Treating cells with **1R-Chl** for 72 hr reduced histone H4 protein by 50%–70%. As controls, we monitored the protein levels of Ras (Figure 3B) and p53 (data not shown) in polyamide-treated and control cells and found no differences. The polyamides were without effect on the transcription of these genes in either microarray or RT-PCR experiments.

To validate *H4c* as the gene target responsible for the growth arrest of SW620 cells, we transfected cells with siRNAs to either *H4c* or to the general housekeeping gene glyceraldehyde-3-phosphate dehydrogenase (*GAPDH*), or with a scrambled sequence siRNA. Cells transfected with *GAPDH* siRNA showed decreased levels of *GAPDH* protein but no change in phenotype and only mild effects on growth (data not shown). The scrambled sequence siRNA was without effect on cell morphology or growth (Figure 3C). In contrast, transfection of *H4c* siRNA under the same conditions caused the same morphology change and similar growth arrest as observed with **1R-Chl**. *H4c* siRNA caused a 73 ( $\pm 5$ )% reduction in cell number after 3 days, whereas **1R-Chl** caused an 85 ( $\pm 5$ )% decrease in cell number over the same time period, relative to the untreated cells. Quantitative RT-PCR confirmed that this siRNA downregulated *H4c* mRNA  $\sim 8.6$ -fold compared to the control, scrambled sequence siRNA. In other experiments, we find that 2-fold downregulation of *H4c* mRNA by siRNA is sufficient to cause growth arrest in SW620 cells. Thus, it appears that inhibition of *H4c* transcription is responsible, at least in part, for the observed change in cellular morphology and growth with **1R-Chl**.

#### Effects of Polyamide **1R-Chl** on Nuclear Structure

SW620 cells were examined by Hoechst staining and fluorescence microscopy after incubation with **1R**- or **1S-Chl** (0.5  $\mu\text{M}$ ) for 72 hr to assess the effects of **1R-Chl** on nuclear structure. Figure 3D demonstrates that **1R-Chl**, but not the inactive polyamide **1S-Chl**, causes the nucleus to enlarge relative to untreated cells. Since previous studies have documented that polyamides targeted to satellite DNA can cause chromatin opening [32], we wished to determine whether the change in

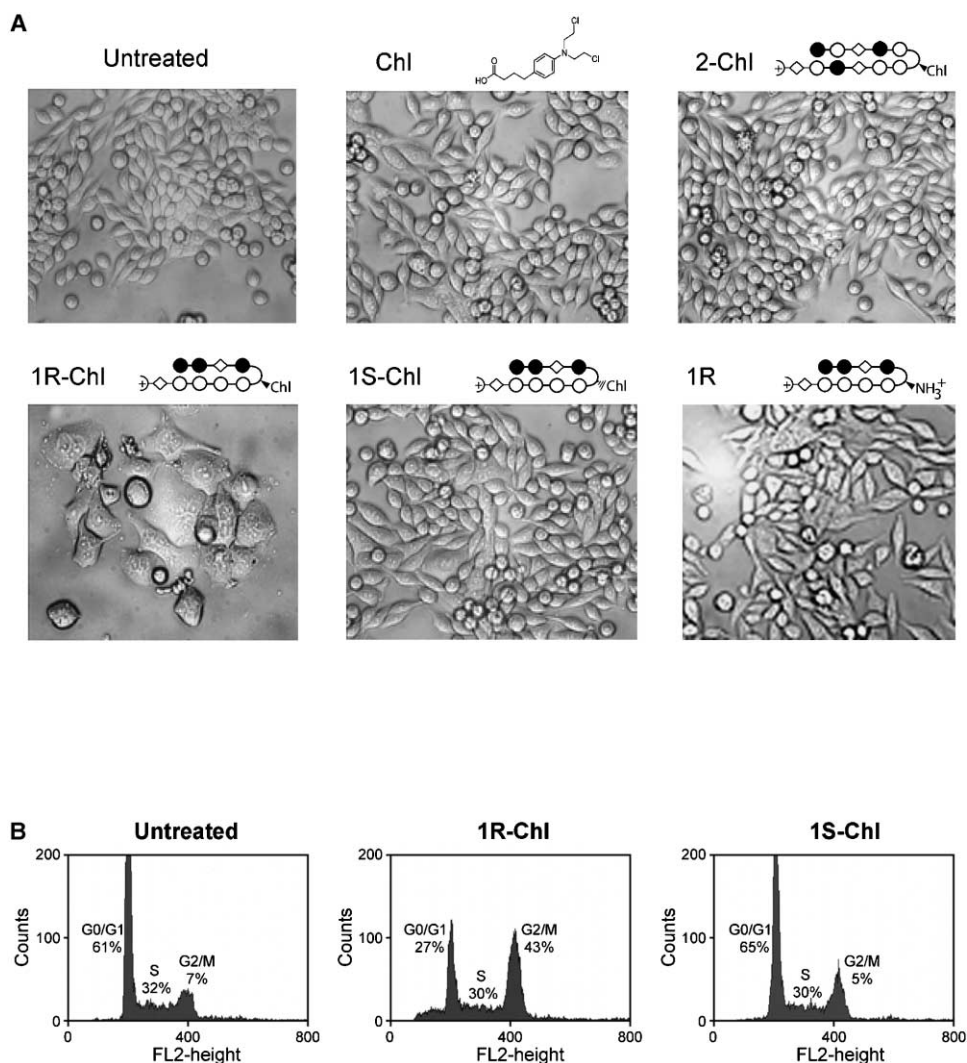


Figure 2. Polyamide **1R-Chl** Specifically Alters the Morphology and Growth of SW620 Cells

(A) Cells were incubated with 0.5  $\mu$ M of the indicated polyamide or **Chl** for 5 days prior to phase microscopy. All images are shown at the same magnification.

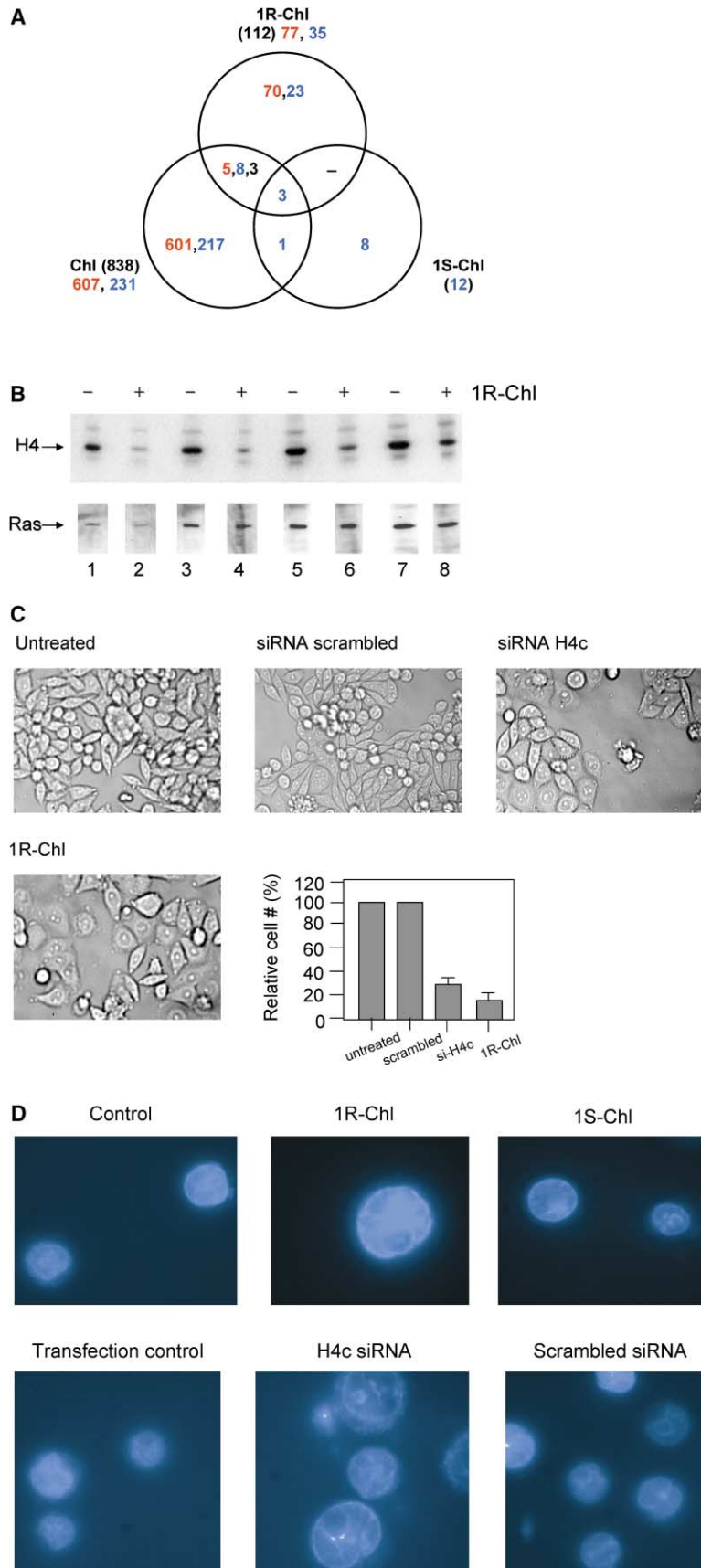
(B) Fluorescence-activated cell-sorting analysis of SW620 cells treated with either no polyamide, 0.5  $\mu$ M **1R-Chl**, or 0.5  $\mu$ M **1S-Chl** for 48 hr prior to staining with propidium iodide (50  $\mu$ g/ml). Cell numbers versus propidium staining are plotted, and the percentages of cells in G0/G1, S, and G2/M phases of the cell cycle are indicated.

nuclear size observed with **1R-Chl** is due to polyamide binding at numerous sites in genomic DNA or to a reduction in H4 protein. SW620 cells were transfected with H4c siRNA or with the scrambled sequence siRNA, and this transfection resulted in only the H4c siRNA causing a similar enlargement of the cell nucleus as **1R-Chl**. This finding indicates that a loss of H4 protein leads to chromatin decondensation and enlargement of the cell nucleus.

#### DNA Binding Properties of the Polyamides

We next explored the DNA binding and alkylation properties of polyamides **1R** and **1S**, and their **Chl** conjugates, with a DNA fragment derived from the human *H4c* gene (isolated by PCR amplification from SW620 genomic DNA). DNase I footprinting was used to monitor the binding specificities and affinities of the parent com-

pounds lacking **Chl**. Previous studies with a polyamide-**Chl** conjugate (where the **Chl** chlorines were replaced with hydroxyls) demonstrated no loss in binding affinities compared to the parent polyamide lacking **Chl** [19]. Although the *H4c* gene contains four match sites for polyamide **1R** (5'-WGGWGW-3', Supplemental Table S2), only two of these sites are occupied in the footprinting experiment (with  $K_d$ s of 0.3 and 0.7 nM; Figure 4A). The two additional match sites are purine tracts, a sequence type that is often poorly bound by hairpin polyamides [13] (Supplemental Table S2). A previous study demonstrated that a polyamide with the turn amino acid *R*-2,4-diaminobutyric acid binds its match site with 170-fold higher affinity than the corresponding *S* enantiomer [30] and documented the importance of the chirality of the hairpin turn in determining binding affinity. As anticipated, the mirror image control **1S** fails



**Figure 3. Identification of the 1R-Chl Gene Target and Effects on Cell Morphology**

(A) Microarray analysis: SW620 cells were treated in triplicate with Chl, 1R-Chl, and 1S-Chl (0.5  $\mu$ M, 72 hr); RNA was isolated and used to probe Affymetrix U133A microarrays. The total numbers of significant genes are shown in parentheses, upregulated genes are shown in red, downregulated genes are shown in blue, and crossed up-down- or down-upregulated populations are shown in black. Shown within each segment of the Venn diagram are the numbers of genes specifically affected by each treatment or common to two or more treatments. Significance analysis was performed as described [39].

(B) Western blot analysis of histone H4 and Ras protein levels in control and polyamide 1R-Chl-treated SW620 cells. Cells were incubated for 72 hr in the presence or absence of 0.5  $\mu$ M polyamide and cell extracts were prepared. For histone H4 detection, the following amounts of acid extract protein were loaded: 1  $\mu$ g (lanes 1 and 2), 2  $\mu$ g (lanes 3 and 4), 3  $\mu$ g (lanes 5 and 6), and 4  $\mu$ g (lanes 7 and 8). For Ras detection, the amounts of total protein were 5  $\mu$ g (lanes 1 and 2), 10  $\mu$ g (lanes 3 and 4), 20  $\mu$ g (lanes 5 and 6), and 30  $\mu$ g (lanes 7 and 8).

(C) siRNA effects on cell morphology and growth. SW620 cells ( $5 \times 10^4$  cells in 250  $\mu$ l culture medium) were transfected with 50 nM of the indicated siRNA or treated with 1R-Chl at 0.5  $\mu$ M, and cells were observed by phase microscopy 72 hr later. Cell numbers, relative to the untreated control, are shown graphically along with standard deviations for three determinations.

(D) Polyamide and siRNA effects on nuclear structure. SW620 cells were either treated with polyamides 1R- or 1S-Chl (0.5  $\mu$ M) or transfected with H4c or scrambled sequence siRNAs and visualized by Hoechst 33342 staining (1  $\mu$ g/ml) 3 days later. A mock transfection was also performed without RNA. All images were acquired and printed at the same magnification.

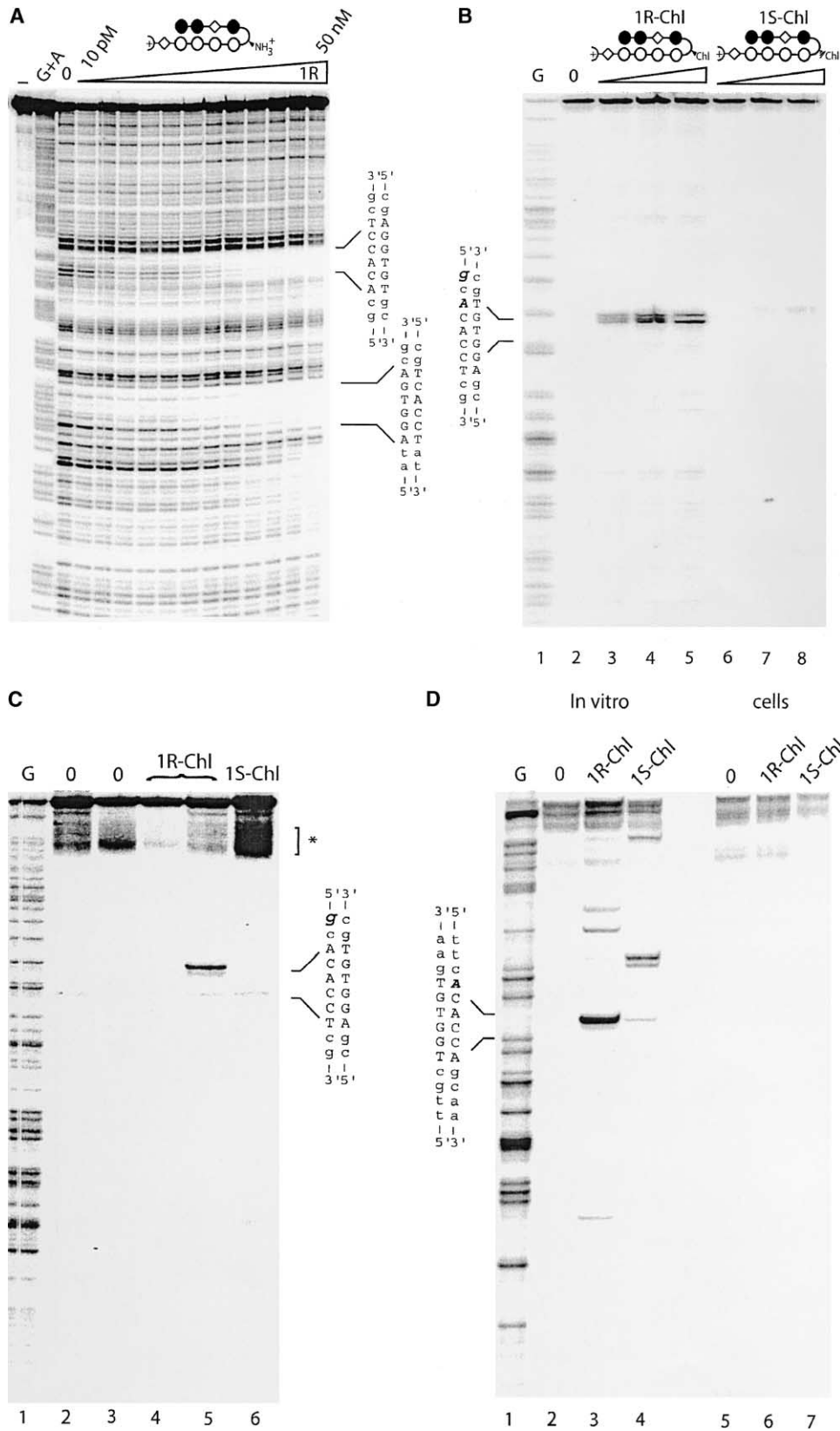


Figure 4. DNA Binding and Alkylation Properties of the Polyamides

(A) Quantitative DNase I footprint analysis for 1R binding to a radiolabeled PCR product derived from the human histone *H4c* gene (labeled on the bottom, template strand). DNA and polyamide were allowed to equilibrate for 16 hr prior to DNase digestion and gel analysis [37]. The

to bind the histone H4c DNA fragment at polyamide concentrations up to 100 nM (data not shown).

Because alkylation of the template strand of the *H4c* gene is more likely to inhibit transcription [26], thermal cleavage assays were used to monitor site-specific alkylation by the polyamide-ChI conjugates on the bottom strand of the H4c PCR product (Figure 4B). Polyamide 1R-ChI alkylates one site in this DNA, corresponding to one of the two match sites described above. Alkylation at the second high-affinity site observed in the footprinting experiment might be prevented by local DNA microstructure. Close inspection of the sequencing gel reveals that alkylation occurs at two nucleotides: the guanine located two bases downstream from the polyamide binding site, and the adenine located proximal to the turn amino acid (Figure 4B). Consistent with the binding experiment, 1S-ChI yields only minor alkylation products, even at the highest polyamide concentration tested (100 nM). Phosphorimage analysis indicates that 1S-ChI exhibits a ~100-fold lower alkylation efficiency than 1R-ChI at this site. No alkylation events were observed with either 1R-ChI or 1S-ChI on the top strand of this PCR product, and polyamides 6-ChI and 7-ChI also fail to significantly alkylate the H4c PCR product on either strand (data not shown). One additional binding site for polyamide 1R is present in the promoter element of the *H4c* gene (5'-TGGTGA-3', located 95 bp upstream from the transcription start site); however, 1R-ChI fails to alkylate this site in vitro (data not shown).

Ligation-mediated PCR was used to monitor alkylation of the coding region of the *H4c* gene in genomic DNA of SW620 cells, and strong alkylation was observed in cellular chromatin (Figure 4C, lane 5). Only the G residue two bases downstream from the polyamide binding site is alkylated in the cell nucleus. In contrast to the in vitro experiment, no alkylation was detected with 1S-ChI in cell culture (lane 6). A control experiment was performed in which the DNA isolation protocol was initiated immediately after the addition of 1R-ChI to the cells. No alkylation was observed under these conditions (lane 4), indicating that alkylation did not occur during DNA isolation and purification. Thus, we have demonstrated direct binding and alkylation of the *H4c* gene by 1R-ChI in live SW620 cells.

We next investigated whether polyamide 1R-ChI alkylates potential target sites in a gene whose transcription is not affected by this compound in SW620 cells. Since 1R-ChI had no effect on *N-Ras* gene expression (as determined in the microarray experiment and confirmed by RT-PCR) or N-Ras protein levels (Figure 3B), we focused on the coding region of this gene. LM-PCR experiments demonstrate that both 1R-ChI and 1S-ChI alkylate sites near the 5' end of this gene in isolated genomic DNA in vitro (on the coding strand; Figure 4D, lanes 3 and 4), but these sites are not available for alkylation in the cell nucleus (lanes 6 and 7). We suspect that differences in chromatin organization between the *H4c* and *N-Ras* genes account for differential polyamide accessibility and the ability of 1R-ChI to regulate expression of these genes.

#### Effects of 1R-ChI on Cell Lines of Different Origin

To assess the generality of the effects of 1R-ChI, we monitored growth rates and viability for various other human cell lines in the absence or presence of conjugates 1R-ChI and 1S-ChI. Polyamide 1S-ChI was without effect on the morphology, viability, or growth of any of ten cell lines tested. In contrast, 1R-ChI showed variable effects in the different lines (Table 2). Based on these results, these cell lines can be divided into three groups: (1) two cell lines in which the compound had no effect up to 1  $\mu$ M concentration (Hep3B hepatocellular carcinoma cells and 293 embryonic kidney cells); (2) three cell lines in which 1R-ChI was growth inhibitory and cytotoxic (22Rv1 prostate, MiaPaCa1 pancreatic, and HeLa cervical carcinoma); and (3) those that responded similarly to SW620 cells, where the growth characteristics of the cells were altered, without apparent cytotoxicity (as assessed by measuring ATP levels). These latter cell lines include two additional colon carcinoma cell lines (SW420 and LoVo), the lymphoblast cell line K562, and SaOS2 osteosarcoma cells (Table 2). Supplemental Figure S3 shows representative results for one cell line in each class. FACS analysis revealed that 1R-ChI had no effect on cell cycle progression in the two unaffected cell lines. In contrast, 1R-ChI blocked cell cycle progression (G2/M arrest) in two out of three cell lines in which the compound was growth inhibitory

---

phosphorimage of the gel is shown, with undigested DNA in the lane marked "-"; a G + A sequencing reaction of the same DNA is shown along with DNase-treated DNA in the absence of polyamide (in the lane marked "0"). Polyamide concentrations were 10 pM, 25 pM, 50 pM, 0.1 nM, 0.25 nM, 0.5 nM, 1 nM, 2.5 nM, 5 nM, 10 nM, 25 nM, and 50 nM.

(B) DNA alkylation by polyamides 1R-ChI and 1S-ChI was monitored for the *H4c* gene PCR product and were analyzed by primer extension to monitor alkylation events on the bottom strand. A G-only sequencing reaction is shown in lane 1. Reactions were incubated in the absence (lane 2) or presence of polyamides at 1, 10, and 100 nM (lanes 3–5 and 6–8, respectively) for 20 hr at 37°C prior to thermal cleavage and gel analysis.

(C) Ligation-mediated PCR analysis for alkylation of the *H4c* gene in SW620 cells [42]. The gel shows a G-only sequencing lane of genomic DNA (lane 1), DNA isolated from cells that were not incubated with polyamide and not subjected to thermal cleavage (lane 2), genomic DNA after thermal cleavage (lane 3), DNA from cells treated with 0.5  $\mu$ M polyamide 1R-ChI for zero time prior to DNA isolation (lane 4), and DNA from cells treated with polyamide 1R-ChI (lane 5) or 1S-ChI (lane 6) at 0.5  $\mu$ M for 24 hr. Nonspecific material present in all lanes is denoted with an asterisk. Polyamide binding site sequences are shown adjacent to each gel, with the binding site in upper case and alkylated bases in bold.

(D) Alkylation of the *N-Ras* gene in genomic DNA in vitro and in SW620 cells. G-only sequencing reaction of genomic DNA (lane 1); genomic DNA was isolated from SW620 cells, digested with the restriction enzyme Hae III, and either subjected to LM-PCR directly (lane 2) or incubated with 0.5  $\mu$ M 1R-ChI (lane 3) or 1S-ChI (lane 4) for 24 hr prior to thermal cleavage and LM-PCR; DNA from cells not treated with polyamide (lane 5) or from cells incubated in culture medium with polyamide 1R-ChI (lane 6) or 1S-ChI (lane 7) at 0.5  $\mu$ M for 24 hr, and treated as for lanes 2–4. The sequence alkylated by 1R-ChI in vitro is shown alongside the figure, with the binding site in upper case and the modified adenine in bold.

Table 2. Effects of Polyamide 1R-ChI on Cell Lines of Different Origin

| Cell Line  | Origin   | Growth Inhibition | Viability <sup>a</sup> | G2/M Cell Cycle Arrest <sup>b</sup> | Relative H4c mRNA <sup>c</sup> | Effect of 1R-ChI on H4c mRNA <sup>d</sup> |
|------------|----------|-------------------|------------------------|-------------------------------------|--------------------------------|---|
| Unaffected |          |                   |                        |                                     |                                |   |
| 293        | kidney   | –                 | +                      | –                                   | 1.13 ± 0.02                    | 0.86 ± 0.01                               |
| Hep3B      | liver    | –                 | +                      | –                                   | 1.16 ± 0.28                    | 1.17 ± 0.28                               |
| Cytotoxic  |          |                   |                        |                                     |                                |   |
| 22Rv1      | prostate | +                 | –                      | –                                   | 0.50 ± 0.04                    | 0.36 ± 0.03                               |
| MiaPaCa1   | pancreas | +                 | –                      | +                                   | 0.12 ± 0.01                    | 0.62 ± 0.06                               |
| HeLa       | cervix   | +                 | –                      | +                                   | 0.25 ± 0.02                    | 0.66 ± 0.04                               |
| Cytostatic |          |                   |                        |                                     |                                |   |
| SW620      | colon    | +                 | +                      | +                                   | 1.00                           | 0.38 ± 0.02                               |
| SW480      | colon    | +                 | +                      | +                                   | 0.38 ± 0.02                    | 0.44 ± 0.02                               |
| LoVo       | colon    | +                 | +                      | ND <sup>e</sup>                     | ND                             | ND  |
| K562       | CML      | +                 | +                      | +                                   | 0.54 ± 0.05                    | 0.23 ± 0.02                               |
| SaOs2      | bone     | +                 | +                      | +                                   | ND                             | ND  |

<sup>a</sup>All assays were performed on cells treated with 1R-ChI at 0.5 μM for 4 days. ATP levels were measured with the ApoSensor assay. “+” indicates ATP levels comparable to untreated cells, while “–” indicates ATP levels below 40% of untreated cells.

<sup>b</sup>As determined by FACS analysis.

<sup>c</sup>H4c mRNA levels (± standard deviation) in untreated cells relative to GAPDH mRNA, normalized to the H4c/GAPDH ratio for SW620 cells, as determined by qRT-PCR.

<sup>d</sup>The values shown represent the ratio of H4c mRNA in the 1R-ChI-treated cells to untreated cells, normalized for GAPDH levels, and are the averages of three determinations (± standard deviation).

<sup>e</sup>Not determined.

and cytotoxic and caused G2/M arrest in each of the cell lines in which the compound was cytostatic (Table 2).

We next monitored the effects of 1R-ChI on H4c mRNA levels in representative cell lines. Polyamide 1R-ChI reduced the level of H4c mRNA in each of the cell lines in which growth inhibition was observed, but it was without effect on H4c mRNA levels in the two unaffected cell lines, 293 and Hep3B (Table 2). We find no correlation between the relative levels of H4c mRNA in untreated cells (relative to the GAPDH control mRNA) and the effects of 1R-ChI on cell proliferation (Table 2). These results were obtained by RT-PCR and were confirmed by Northern blotting (data not shown).

#### Tumorigenicity of SW620 Cells Treated with Polyamide 1R-ChI

To assess the potential tumorigenicity of polyamide 1R-ChI-treated versus untreated cells, we employed a standard soft-agar assay, in which equal numbers of untreated and polyamide-treated cells were inoculated into soft agar (without polyamide) and grown for up to 2 weeks (Figure 5A). Untreated cells and cells treated with control compounds (1S-ChI, parent 1R, and ChI) formed colonies in this assay, whereas cells pretreated with 1R-ChI failed to grow, although trypan blue exclusion indicated that the cells were viable. This suggests that 1R-ChI converts these cells to an irreversible nontumorigenic phenotype. Moreover, and similar to the morphological change observed in standard cell culture conditions, growth arrest required both a specific polyamide DNA binding domain and the ChI alkylating moiety.

To determine whether this loss of anchorage-independent growth reflects a loss of tumorigenicity in vivo,

we performed animal studies in athymic nude-nu mice. SW620 cells were either untreated (group 1), treated for 3 days with 0.5 μM polyamide 1R-ChI (group 2), or treated with 1S-ChI (group 3). The cells were then washed and suspended in polyamide-free PBS, and cells were injected in groups of five nude mice (1 × 10<sup>7</sup> cells/mouse). Each of the mice in groups 1 and 3 developed tumors measuring ~1–1.5 cm after 23 days, whereas none of the mice in group 2 developed tumors. As a more stringent test of the efficacy of this compound, we injected groups of five nude mice with SW620 cells and then treated the animals with polyamides. After 1 week, when tumors began to form, mice were injected intravenously with 200 μl of either PBS or polyamide 1R-ChI (in PBS), followed by a subsequent injection after 3 days. After 28 days, the animals were euthanized, and tumors were dissected and weighed (Figure 5B, Experiment 1). Polyamide treatment substantially suppressed tumor growth, in a dose-dependent manner. Mice that had been injected with 30 and 120 nmoles of 1R-ChI had tumors that weighed an average of 35% and 16%, respectively, of the tumors of control mice. In a second experiment, mice were again injected with SW620 cells, tumors were allowed to establish, and tumor volumes were determined prior to polyamide treatment and at 15 days post-treatment. Three doses of polyamide 1R-ChI (120 nmol, administered on treatment days 0, 2, and 4) prevented any significant increase in tumor volume, whereas mice receiving a similar dosing regimen of polyamide 1S-ChI developed tumors comparable to the untreated control animals (Figure 5B, Experiment 2). Importantly, no obvious toxicity was associated with polyamide treatment in vivo at a polyamide concentration and dosing regimen at which the therapeutic result was obtained.



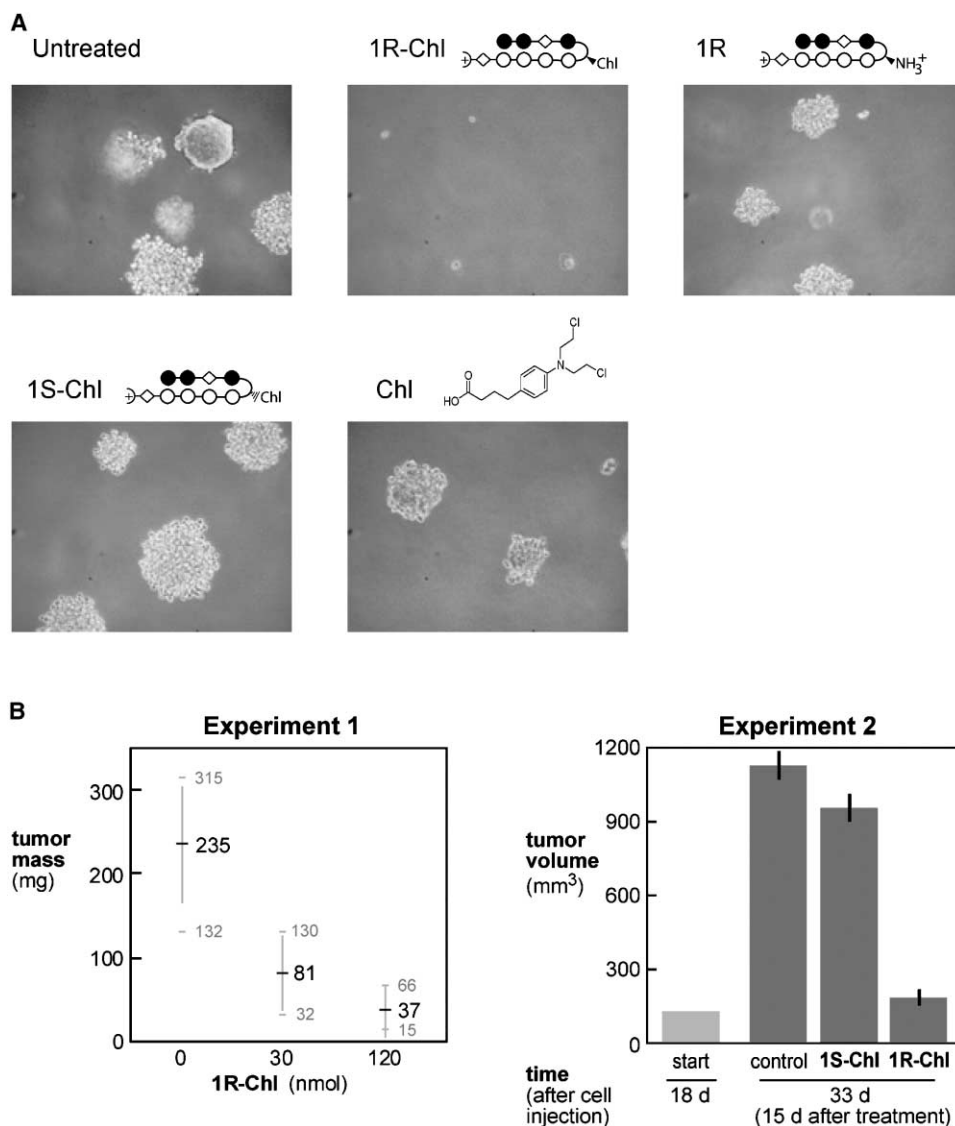


Figure 5. Polyamide 1R-Chl Abolishes Anchorage-Independent Growth In Vitro and Tumorigenicity of SW620 Cells in Nude Mice

(A) Soft agar assay: cells were treated with 0.5  $\mu$ M of the indicated polyamide or Chl for 5 days prior to soft agar inoculation, in the absence of polyamide, and visualized by microscopy 7 days later. Note the clusters of cells in all panels except for that showing cells treated with polyamide 1R-Chl, in which only individual cells are seen.

(B) Effect of polyamide 1R-Chl on tumor growth in athymic nude-nu mice. In Experiment 1, the tumor weight at 28 days postinjection of  $1 \times 10^7$  SW620 cells is indicated as mean, range of observed values, and standard deviation (vertical line) for each group of five treated or untreated mice. In Experiment 2, tumor volumes were determined 18 days postinjection of SW620 cells and at 15 days posttreatment (day 33) with 120 nmole of 1R-Chl or 1S-Chl, as described in the text. Mean and standard deviations for four mice are indicated.

## Discussion

We have shown that a specific pyrrole-imidazole polyamide-chlorambucil conjugate, 1R-Chl, alters the morphology of SW620 cells and causes these cells to arrest at the G2/M stage of the cell cycle, without apparent cytotoxicity. While two cell lines were not affected by this polyamide (293 and Hep3B cells), eight cell lines exhibited growth arrest when treated with 1R-Chl. Of this latter class of cells, 1R-Chl was cytotoxic in some cell lines and cytostatic in others. The molecular basis for these differences awaits further investigation. Mi-

croarray analysis revealed that a limited number of genes are specifically downregulated by 1R-Chl in SW620 cells, and only one gene (histone *H4c*) is downregulated by  $\sim 2$ -fold, even though potential binding sites for this polyamide are present thousands of times in the human genome. RT-PCR and Western blotting experiments confirm that histone H4 mRNA and protein are indeed downregulated by this polyamide. Although we cannot rule out the possibility that other down- (or up) regulated genes contribute to the cellular responses induced by 1R-Chl, downregulation of the H4c gene with siRNA was also sufficient to induce similar morpho-

logical and growth changes as polyamide **1R-ChI**. It will be of interest to determine whether the gene expression profile of cells treated with H4c siRNA is similar to that of **1R-ChI**-treated cells. Strikingly, each of the cell lines in which growth arrest was observed also showed downregulation of H4c mRNA. No downregulation of H4c mRNA was observed in the two cell lines in which growth arrest was not observed (Table 2).

Since the active molecule is a DNA alkylator, one could argue that the DNA damage response is involved in the observed cellular responses to **1R-ChI** in SW620 cells; however, we did not observe upregulation of stress response genes with **1R-ChI**, as we observed with free chlorambucil, nor did we observe large numbers of apoptotic cells. DNA damaging agents induce apoptosis, which would have been detected in our ATP assays and by FACS analysis. Only a small fraction of **1R-ChI**-treated cells are apoptotic (as shown in the FACS analysis, Figure 2B). Thus, growth arrest with **1R-ChI** is unlikely to be due to DNA damage, at least in cells in which this compound is cytostatic. Taken together, our results suggest that downregulation of the *H4c* gene by **1R-ChI** (by only ~2-fold) contributes to block cell cycle progression and tumorigenicity.

The human genome encodes 14 genes encoding the same H4 protein (at the level of the primary amino acid sequence); however, only *H4c* was affected by the polyamide. Inspection of our microarray data indicates that *H4c* is the most highly expressed histone H4 gene in SW620 cells, accounting for ~70% of total H4 mRNA. Other microarray data [33] indicate that this gene is highly expressed in several, but not all, cancer cell lines, and that expression of this gene is higher in cancer cells than in normal human tissues and cell types. Indeed, histone *H4c* expression is far lower in normal human kidney tissue and in peripheral blood lymphocytes than in SW620 cells and accounts for less than 20% of the total H4 mRNA in kidney or lymphocytes. Whereas sequence analysis reveals that binding sites for polyamide **1R** are present in all members of this gene family, only the *H4c* gene was affected by polyamide **1R-ChI**; thus, it is likely that the high expression level and active chromatin structure marks the *H4c* gene as an available polyamide target. The inability of **1R-ChI** to downregulate H4c mRNA transcription in 293 and Hep3B cells could be due to either a different chromatin structure of the *H4c* gene in these cells compared to the other cell lines examined (such as a difference in nucleosome positioning) or to the nuclear localization properties of the ligand in these cell lines [15, 16]. Future studies will address this issue.

Downregulation of a key component of chromatin is consistent with our observation that cells treated with **1R-ChI** are blocked in the G2/M phase of the cell cycle. Cells that are unable to form their full complement of nucleosomes during DNA replication will not be able to condense their DNA into mitotic chromosomes and hence will be unable to proceed through mitosis. Reduction in histone H4 mRNA (and protein) observed with either **1R-ChI** or H4c siRNA and enlargement of the cell nucleus are consistent with decondensation of nuclear chromatin. Cell cycle arrest has previously been observed by downregulation of H4 transcription in human

cell lines, mediated by antisense ablation of the mRNA for the histone gene transcription factor HiNF-P [34]. This finding is similar to our finding that downregulation of H4c mRNA by siRNA causes growth arrest. It was surprising that downregulation of histone H4 did not have a global effect on genomic transcription, because chromatin structure is thought to be central to regulation of gene expression in eukaryotic cells. In contrast, depletion of H4 protein by a genetic approach in yeast revealed that expression of 15% of the genome was increased and expression of 10% of genes was decreased [35, 36]. The molecular basis for this difference between yeast and human cells remains to be elucidated.

### Significance

**We report the sequence-specific silencing of an endogenous cellular gene, the human histone H4c gene, with a polyamide-chlorambucil conjugate. Direct evidence that the ligand occupies its chromatin target site in live cells was obtained by ligation-mediated PCR. We also provide target validation by siRNA. Surprisingly, downregulation of histone H4 protein, a key component of chromatin, does not lead to large global changes in gene expression. Cells treated with polyamide **1R-ChI** fail to grow in soft agar and do not form tumors in nude mice, indicating that polyamide-treated cells are no longer tumorigenic and have entered an irreversible cellular pathway. Importantly, this compound also blocks tumorigenicity of metastatic colon carcinoma cells when administered by intravenous injection in immunocompromised mice. It is likely that this compound will be active in vivo against cancer cell types in which the *H4c* gene is downregulated by the polyamide in vitro. Our results suggest that histone *H4c* may be a new target in human cancer biology and that screening cells with programmable molecules may be a useful approach for uncovering new gene targets.**

### Experimental Procedures

#### Polyamide Synthesis and Characterization

Polyamides were synthesized by using solid phase methods [29], and the identity and purity of the compounds was established by analytical HPLC and mass spectrometry (MALDI-TOF-MS). For polyamide conjugates, the free amine of the precursor polyamide (at the  $\alpha$  position of the turn amino acid) was reacted with the activated esters of either Bodipy FL (succinimidyl ester, Molecular Probes) [14] or ChI (carboxylic acid precursor from Sigma, OBt ester generated from chlorambucil and HBTU under standard conditions [19]), and the conjugates were purified by reversed phase HPLC.

Binding affinities of the unconjugated polyamides were determined by quantitative DNase I footprinting [37] with a radiolabeled PCR product derived from the human histone *H4c* gene (accession number NM\_003542). A 214 bp region of mRNA-coding sequence was amplified from SW620 cell genomic DNA with PCR primers corresponding to nucleotide positions 71–90 and 265–284 and was radiolabeled by the inclusion of one 5' end-labeled primer (labeled with T4 polynucleotide kinase and  $\gamma$ -<sup>32</sup>P-ATP) in the PCR reaction. Formic acid (0.3% for 25 min at 37°C) was used to generate A + G sequence markers, and dimethylsulfate (2% for 2 min at 23°C) was used for the G-only reaction [38]. Alkylation reactions on the unlabeled PCR product were carried out with polyamide-ChI conjugates for 20 hr at 37°C, followed by thermal cleavage [19], and alkylation

sites were mapped by primer extension with the radiolabeled top strand primer, unlabeled dNTPs, and Vent polymerase (New England Biolabs). Footprinting and alkylation reactions were analyzed by electrophoresis on 6% sequencing polyacrylamide gels containing 8.3 M urea and 88 mM Tris-borate (pH 8.3), 2 mM EDTA. Quantitation of the footprint titrations was by phosphorimage analysis with a Molecular Dynamics SF PhosphorImager with Kodak Phosphor Screens (SO 230) and ImageQuant software.

#### Cell Culture

The human colon adenocarcinoma cell lines SW480 (American Type Culture Collection [ATCC] CCL-228), SW620 (CCL-227; derived from a lymph node metastasis from the same patient as SW480), and LoVo (CL-229) were maintained in Leibovitz medium as recommended by the ATCC. Other cell lines were obtained from ATCC and were maintained as recommended. Cell growth and morphology were monitored by phase contrast microscopy, and viability was monitored by trypan blue exclusion and an ATP assay (ApoSENSOR, BioVision). Deconvolution microscopy with polyamide-bodipy conjugates was performed as described [17]. For Hoechst staining, cells were first trypsinized, washed in PBS, and stained with Hoechst 33342 (1  $\mu$ g/ml) prior to fluorescence microscopy. The effects of polyamide-alkylator conjugates on cell cycle progression were monitored by FACS analysis after staining with propidium iodide (50  $\mu$ g/ml). Synthetic double-stranded siRNAs targeting the histone *H4c* gene, the *GAPDH* gene, and a scrambled sequence siRNA, were obtained in HPLC-purified and annealed form from Ambion. The *H4c* sense sequence was as follows, with single-stranded nucleotides in lower case: 5'-GGGCAUUACAAAACCGCUTt-3'. SW620 cells ( $5 \times 10^4$  cells per well) were transfected with 50 nM siRNA by using the Silencer siRNA Transfection Kit (Ambion).

#### Soft Agar Assays

Soft agar assays were performed in 6-well culture dishes by using SeaPlaque low-melting temperature agarose (Cambrex Bio Science Rockland, Inc.). The cell growth medium was supplemented with 20% fetal bovine serum. Cells were treated for 5 days with or without polyamide, harvested by trypsin treatment, and counted by using a hemocytometer. Cell viability was higher than 90% in both treated and untreated cells, as determined by trypan blue exclusion assays. A total of  $3 \times 10^3$  cells of each sample were suspended in 0.5 ml growth medium and transferred to a sterile tube containing 2 ml of a 0.375% agarose suspension in medium. Cells were gently mixed by pipetting and quickly transferred to the culture dish containing a thin layer (0.5 ml) of solidified 0.5% agarose in medium. Cultures were incubated for 1–2 weeks prior to visualization by microscopy.

#### Affymetrix Oligonucleotide Arrays

Total RNA from SW620 cells from four pooled culture wells from triplicate experiments was isolated by using a Qiagen RNeasy Midi Kit according to the manufacturer's instructions. Microarray experiments were performed at the DNA Array Core Facility of The Scripps Research Institute by using Affymetrix Genechip Human Genome U133A chips. Genechip data were analyzed with Affymetrix Micro-Array Suite (MAS 5.0) software. RMA values for probe sets of triplicate experiments were compared to control values by using Significance Analysis of Microarrays (SAM) 1.21 [39], and a false discovery rate of one gene was allowed per experimental condition.

#### Real-Time Quantitative RT-PCR

Real-time quantitative RT-PCR analysis was performed essentially as previously described [40], by using the primers described above for the *H4c* gene. RNA was standardized by quantification of *GAPDH* mRNA [41]. Real-time quantitative RT-PCR was performed by using Quantitect SYBR Green RT-PCR (Qiagen) [17]. Statistical analysis was performed on three independent quantitative RT-PCR experiments for each RNA sample.

#### Western Blot Analysis

Protein levels in polyamide-treated and untreated cells were monitored by Western blotting with antibodies to histone H4 (Upstate Biotechnology) or with control antibodies to Ras (Oncogene Sciences) and p53 (Upstate). Histones were purified by acid extraction

as described in the protocols provided by Upstate Biotechnology. Signals were detected by chemiluminescence after probing the blot with HRP-conjugated secondary antibody (Supersignal West, Pierce). To quantify the relative levels of proteins, autoradiograms (within the linear response range of X-ray film) were converted into digital images, and the signals were quantified with ImageQuant software.

#### Ligation-Mediated PCR

Polyamides were added to approximately  $2 \times 10^7$  SW620 cells and incubated at 37°C for 24 hr or subjected to DNA isolation immediately after the addition of polyamides. Genomic DNA was extracted by using a Qiagen genomic extraction kit. DNA samples were digested with appropriate restriction enzymes (DraI for *H4c* and HaeIII for *N-Ras*) and were subjected to thermal cleavage in 10 mM sodium citrate or in 1 M piperidine [19]. To generate a sequence marker, DNA (50  $\mu$ g) was incubated with dimethylsulfate (0.5% for 2 min), and then treated with 1 M piperidine for 30 min at 95°C. DNA samples were precipitated with ethanol twice and were used in ligation-mediated PCR with nested primers according to Garrity and Wold [42]. First-strand synthesis was by primer extension with Vent polymerase, with a primer corresponding to nucleotide positions 44–63 on the top strand of the *H4c* gene (NM\_003542) or with a primer corresponding to nucleotide positions 88,793–88,812 on the top strand of the *N-Ras* gene (AL096773.6.1.140207). The double-stranded linker sequence and linker ligation were performed as described [42]. A total of 35 cycles of PCR (with the gene-specific primer and one linker primer) was followed by primer extension with a radiolabeled primer, corresponding to nucleotide positions 71–90 on the top strand of the *H4c* gene or to positions 88,822–88,842 on the top strand of the *N-Ras* gene. The final radiolabeled DNA was analyzed on a sequencing gel.

#### Animal Experiments

Female athymic nude-nu mice were purchased from The Scripps Research Institute Division of Animal Resources. Experimental protocols were approved by the Scripps Institutional Animal Welfare Committee and are described in the text and figure legends.

#### Supplemental Data

Supplemental Data including data on polyamide effects on various cell lines and the detailed Affymetrix microarray data for the effects of polyamides on global transcription are available at <http://www.chembiol.com/cgi/content/full/11/11/1583/DC1/>.

#### Acknowledgments

We thank Peter Vogt, Ernest Beutler, and Thomas Dueel for discussions and advice; Steve Head and members of the Scripps Microarray Core facility for assistance with gene profiling studies; Malcolm Wood for help with deconvolution microscopy; Daniel Salomon for access to human microarray data; Caren Lund for FACS analysis; and Veronique Blais and David Alvarez for microscopy. This work was supported by grants from the National Institutes of Health. B.S.E. was supported by a predoctoral fellowship from the Howard Hughes Medical Institute, and R.B. was supported by National Institute of Health postdoctoral training grant T32 AI07354. J.M.G. and P.B.D. dedicate this work to the memory of Francis Crick.

Received: August 4, 2004

Revised: September 3, 2004

Accepted: September 9, 2004

Published: November 29, 2004

#### References

1. Opalinska, J.B., and Gewirtz, A.M. (2002). Nucleic-acid therapeutics: basic principles and recent applications. *Nat. Rev. Drug Discov.* 1, 503–514.
2. Braasch, D.A., and Corey, D.R. (2002). Novel antisense and peptide nucleic acid strategies for controlling gene expression. *Biochemistry* 41, 4503–4510.
3. Scherer, L.J., and Rossi, J.J. (2003). Approaches for the se-

- quence-specific knockdown of mRNA. *Nat. Biotechnol.* **21**, 1457–1465.
- Choo, Y., Sanchez-Garcia, I., and Klug, A. (1994). In vivo repression by a site-specific DNA-binding protein designed against an oncogenic sequence. *Nature* **372**, 642–645.
  - Beerli, R.R., Dreier, B., and Barbas, C.F., 3rd. (2000). Positive and negative regulation of endogenous genes by designed transcription factors. *Proc. Natl. Acad. Sci. USA* **97**, 1495–1500.
  - Reynolds, L., Ullman, C., Moore, M., Isalan, M., West, M.J., Clapham, P., Klug, A., and Choo, Y. (2003). Repression of the HIV-1 5' LTR promoter and inhibition of HIV-1 replication by using engineered zinc-finger transcription factors. *Proc. Natl. Acad. Sci. USA* **100**, 1615–1620.
  - Papworth, M., Moore, M., Isalan, M., Minczuk, M., Choo, Y., and Klug, A. (2003). Inhibition of herpes simplex virus 1 gene expression by designer zinc-finger transcription factors. *Proc. Natl. Acad. Sci. USA* **100**, 1621–1626.
  - Rebar, E.J., Huang, Y., Hickey, R., Nath, A.K., Meoli, D., Nath, S., Chen, B., Xu, L., Liang, Y., Jamieson, A.C., et al. (2002). Induction of angiogenesis in a mouse model using engineered transcription factors. *Nat. Med.* **8**, 1427–1432.
  - Qin, X.F., An, D.S., Chen, I.S., and Baltimore, D. (2003). Inhibiting HIV-1 infection in human T cells by lentiviral-mediated delivery of small interfering RNA against CCR5. *Proc. Natl. Acad. Sci. USA* **100**, 183–188.
  - Gottesfeld, J.M., Neely, L., Trauger, J.W., Baird, E.E., and Dervan, P.B. (1997). Regulation of gene expression by small molecules. *Nature* **387**, 202–205.
  - Denison, C., and Kodadek, T. (1998). Small-molecule-based strategies for controlling gene expression. *Chem. Biol.* **5**, 129–145.
  - Dervan, P.B. (2001). Molecular recognition of DNA by small molecules. *Bioorg. Med. Chem.* **9**, 2215–2235.
  - Dervan, P.B., and Edelson, B.S. (2003). Recognition of the DNA minor groove by pyrrole-imidazole polyamides. *Curr. Opin. Struct. Biol.* **13**, 284–299.
  - Belitsky, J.M., Leslie, S.J., Arora, P.S., Beerman, T.A., and Dervan, P.B. (2002). Cellular uptake of N-methylpyrrole/N-methylimidazole polyamide-dye conjugates. *Bioorg. Med. Chem.* **10**, 3313–3318.
  - Best, T.P., Edelson, B.S., Nichols, N.G., and Dervan, P.B. (2003). Nuclear localization of pyrrole-imidazole polyamide-fluorescein conjugates in cell culture. *Proc. Natl. Acad. Sci. USA* **100**, 12063–12068.
  - Edelson, B.S., Best, T.P., Olenyuk, B., Nickols, N.G., Doss, R.M., Foister, S., Heckel, A., and Dervan, P.B. (2004). Influence of structural variation on nuclear localization of DNA-binding polyamide-fluorophore conjugates. *Nucleic Acids Res.* **32**, 2802–2818.
  - Dudouet, B., Burnett, R., Dickinson, L.A., Wood, M.R., Melander, C., Belitsky, J.M., Edelson, B., Wurtz, N., Briehn, C., Dervan, P.B., et al. (2003). Accessibility of nuclear chromatin by DNA binding polyamides. *Chem. Biol.* **10**, 859–867.
  - Gottesfeld, J.M., Belitsky, J.M., Melander, C., Dervan, P.B., and Luger, K. (2002). Blocking transcription through a nucleosome with synthetic DNA ligands. *J. Mol. Biol.* **321**, 249–263.
  - Wurtz, N.R., and Dervan, P.B. (2000). Sequence specific alkylation of DNA by hairpin pyrrole-imidazole polyamide conjugates. *Chem. Biol.* **7**, 153–161.
  - Weiss, G.R., Poggesi, I., Rocchetti, M., DeMaria, D., Mooneyham, T., Reilly, D., Vitek, L.V., Whaley, F., Patricia, E., Von Hoff, D.D., et al. (1998). A phase I and pharmacokinetic study of tallimustine [PNU 152241 (FCE 24517)] in patients with advanced cancer. *Clin. Cancer Res.* **4**, 53–59.
  - Boger, D.L., Searcey, M., Tse, W.C., and Jin, Q. (2000). Bifunctional alkylating agents derived from duocarmycin SA: potent antitumor activity with altered sequence selectivity. *Bioorg. Med. Chem. Lett.* **10**, 495–498.
  - Chang, A.Y., and Dervan, P.B. (2000). Strand selective cleavage of DNA by diastereomers of hairpin polyamide-seco-CBI conjugate. *J. Am. Chem. Soc.* **122**, 4856–4864.
  - Shinohara, K., Narita, A., Oyoshi, T., Bando, T., Teraoka, H., and Sugiyama, H. (2004). Sequence-specific gene silencing in mammalian cells by alkylating pyrrole-imidazole polyamides. *J. Am. Chem. Soc.* **126**, 5113–5118.
  - Smellie, M., Bose, D.S., Thompson, A.S., Jenkins, T.C., Hartley, J.A., and Thurston, D.E. (2003). Sequence-selective recognition of duplex DNA through covalent interstrand cross-linking: kinetic and molecular modeling studies with pyrrolbenzodiazepine dimers. *Biochemistry* **42**, 8232–8239.
  - Kumar, R., and Lown, J.W. (2003). Recent developments in novel pyrrolo[2,1-c][1,4]benzodiazepine conjugates: synthesis and biological evaluation. *Mini Rev. Med. Chem.* **3**, 323–339.
  - Oyoshi, T., Kawakami, W., Narita, A., Bando, T., and Sugiyama, H. (2003). Inhibition of transcription at a coding sequence by alkylating polyamide. *J. Am. Chem. Soc.* **125**, 4752–4754.
  - Wang, Y.D., Dziegielewska, J., Wurtz, N.R., Dziegielewska, B., Dervan, P.B., and Beerman, T.A. (2003). DNA crosslinking and biological activity of a hairpin polyamide-chlorambucil conjugate. *Nucleic Acids Res.* **31**, 1208–1215.
  - Leibovitz, A., Stinson, J.C., McCombs, W.B., III, McCoy, C.E., Mazur, K.C., and Mabry, N.D. (1976). Classification of human colorectal adenocarcinoma cell lines. *Cancer Res.* **36**, 4562–4569.
  - Baird, E.E., and Dervan, P.B. (1996). Solid phase synthesis of polyamides containing imidazole and pyrrole amino acids. *J. Am. Chem. Soc.* **118**, 6141–6146.
  - Herman, D.M., Baird, E.E., and Dervan, P.B. (1998). Stereochemical control of the DNA binding affinity, sequence specificity, and orientation preference of chiral hairpin polyamides in the minor groove. *J. Am. Chem. Soc.* **120**, 1382–1391.
  - Melander, C., Herman, D.M., and Dervan, P.B. (2000). Discrimination of A/T sequences in the minor groove of DNA within a cyclic polyamide motif. *Chemistry* **6**, 4487–4497.
  - Janssen, S., Durussel, T., and Laemmli, U.K. (2000). Chromatin opening of DNA satellites by targeted sequence-specific drugs. *Mol. Cell* **6**, 999–1011.
  - The Genomics Institute of the Novartis Research Foundation. (2004). Gene Expression Atlas (<http://expression.gnf.org>).
  - Mitra, P., Xie, R.L., Medina, R., Hovhannisyan, H., Zaidi, S.K., Wei, Y., Harper, J.W., Stein, J.L., van Wijnen, A.J., and Stein, G.S. (2003). Identification of Hinf-P, a key activator of cell cycle-controlled histone H4 genes at the onset of S phase. *Mol. Cell Biol.* **23**, 8110–8123.
  - Kim, U.J., Han, M., Kayne, P., and Grunstein, M. (1988). Effects of histone H4 depletion on the cell cycle and transcription of *Saccharomyces cerevisiae*. *EMBO J.* **7**, 2211–2219.
  - Wyrick, J.J., Holstege, F.C., Jennings, E.G., Causton, H.C., Shore, D., Grunstein, M., Lander, E.S., and Young, R.A. (1999). Chromosomal landscape of nucleosome-dependent gene expression and silencing in yeast. *Nature* **402**, 418–421.
  - Trauger, J.W., and Dervan, P.B. (2001). Footprinting methods for analysis of pyrrole-imidazole polyamide/DNA complexes. *Methods Enzymol.* **340**, 450–466.
  - Maxam, A., and Gilbert, W. (1980). Sequencing end-labeled DNA with base-specific chemical cleavages. *Methods Enzymol.* **65**, 497–559.
  - Tusher, V.G., Tibshirani, R., and Chu, G. (2001). Significance analysis of microarrays applied to the ionizing radiation response. *Proc. Natl. Acad. Sci. USA* **98**, 5116–5121.
  - Chuma, M., Sakamoto, M., Yamazi, K., Ohta, T., Ohki, M., Asaka, M., and Hirohashi, S. (2003). Expression profiling in multistage hepatocarcinogenesis: identification of HSP70 as a molecular marker of early hepatocellular carcinoma. *Hepatology* **37**, 198–207.
  - Pattyn, F., Speleman, F., De Paepe, A., and Vandesompele, J. (2003). RTPPrimerDB: the real-time PCR primer and probe database. *Nucleic Acids Res.* **31**, 122–123.
  - Garrity, P.A., and Wold, B.J. (1992). Effects of different DNA polymerases in ligation-mediated PCR: enhanced genomic sequencing and in vivo footprinting. *Proc. Natl. Acad. Sci. USA* **89**, 1021–1025.